Korean J. Chem. Eng., 33(7), 2235-2239 (2016)
DOI: 10.1007/s11814-016-0077-7

pISSN: 0256-1115
eISSN: 1975-7220

Electrolytic reduction rate of porous UO_2 pellets

Min Ku Jeon*,,†, Eun-Young Choi*, Sung-Wook Kim*,**, Sang-Kwon Lee*, Hyun Woo Kang*, Sun Seok Hong*, Jeong Lee*, Jin-Mok Hur*, Sang-Chae Jeon*, Ju Ho Lee*, Yung-Zun Cho*,**, and Do-Hee Ahn*,****

*Nuclear Fuel Cycle Process Development Division, Korea Atomic Energy Research Institute, 989-111 Daedeok-daero, Yuseong-gu, Daejeon 34059, Korea
**Department of Quantum Energy Chemical Engineering, University of Science and Technology, 217 Gajeong-ro, Yuseong-gu, Daejeon 34113, Korea
(*Received 10 January 2016 • accepted 10 March 2016*)

Abstract−The electrolytic reduction rate of porous UO_2 pellets in a LiCl salt was investigated for various applied charges. The degree of reduction (α) value was evaluated from the ratios of cross-sectional areas of the reduced and oxide parts. An analysis of the experimental results revealed that the first-order reaction model is the best geometry function to describe the reduction reaction. An electrolytic reduction rate equation was proposed using the first-order model, although it was available in a limited region of ($0 \le \alpha \le 0.56$). A power law based reaction rate equation was also suggested for the whole range of α, and the reaction time for a complete reduction, estimated using the power law equation, was confirmed through the experimental results. Changes in the Li-Li_2O concentration around the reduced pellets for various applied charges were also measured, which increased up to 23 wt% with increasing α.

Keywords: Electrolytic Reduction, Reaction Rate, Pyroprocessing, Uranium Dioxide, Reaction Model

INTRODUCTION

Electrolytic reduction (ER) of uranium dioxide is a key technique that enables an application of oxide fuels in pressurized water reactors (PWRs) to a previously proven electro-refining process [1]. The Republic of Korea (ROK) is operating 24 nuclear reactors, and 20 of them are PWRs employing low-enriched UO_2 as a fuel. The 20 PWRs are producing about 300 tons of used nuclear fuel (UNF) every year, which contains highly toxic nuclides such as plutonium and americium. Currently, there are no proven technologies that can completely separate the UNFs from the biosphere, and each country is looking for its own way including deep bore hole disposal, interim storage, and recycling as a mixed oxide fuel [2]. In the ROK, UNFs are currently stored in storage pools located in reactor sites, and old pools are facing their capacity limit in several years [3]. Naturally, the government of the ROK is looking for a solution to manage UNFs, and pyroprocessing is proposed as a suitable technology for this purpose [4,5]. The well-known wet reprocessing technique employs nitric acid based solution extraction processes, and is also known as an efficient way to extract pure plutonium, which is a source of nuclear bombs. In other words, the wet reprocessing is not an option for the ROK owing to nuclear nonproliferation treaty (NPT), and pyroprocessing is known as a proliferation resistant technology. The pyroprocessing employs electrochemical reactions, and plutonium is co-recovered with uranium and other transuranic nuclides during the electro-winning process. The recycling of metal fuels in fast reactors using pyroprocessing was demonstrated in the US through the EBR-II (Experimental Breeder Reactor-II) project [1], and a linkage between the PWR oxide fuel and metal fuel pyroprocessing is the ER technique.

The ER process was inspired by the research of Chen's group [6], which demonstrated direct reduction of TiO_2 into Ti by an electrochemical reaction. However, it is believed that the ER process includes a chemical reaction as noted below [7]:

Cathode: $2Li_2O + 4e^- \rightarrow 4Li + 2O^{2-}$ (electrochemical rxn.)
$4Li + UO_2 \rightarrow 2Li_2O + U$ (chemical rxn.)
Anode: $2O_2^- \rightarrow O_2\,(g) + 4e^-$ (electrochemical rxn.)

The best merit of the ER process is the internal recycling of Li_2O, meaning that the addition of Li_2O is not necessary during the reaction. The Korea Atomic Energy Research Institute (KAERI) has been working on the ER process and achieved promising results [7-12]. Nowadays, a scale-up of the ER process is an issue at KAERI to achieve a throughput of 50 kg U/day. Various types of data including the effects of reactor shape, size of the UO_2 basket, and distance between the anode and cathode electrodes are required to successfully build a scaled-up electrochemical system. However, it is hard to find a systematic approach on the electrolytic reduction rate of UO_2, although it is a starting point in estimating the reaction time and efficiency of a scaled-up system. In the present study, the reduction rate of UO_2 was investigated to achieve a reduction rate equation so that it can provide useful information for the scale-up design. In addition, the concentration of Li-Li_2O was measured to identify the actual amount of Li-Li_2O around the pellets, because it might reveal the actual concentration of Li-Li_2O that participates in the reduction reaction and more precise informa-

†To whom correspondence should be addressed.
E-mail: minku@kaeri.re.kr
‡This article is dedicated to Prof. Seong Ihl Woo on the occasion of his retirement from KAIST.

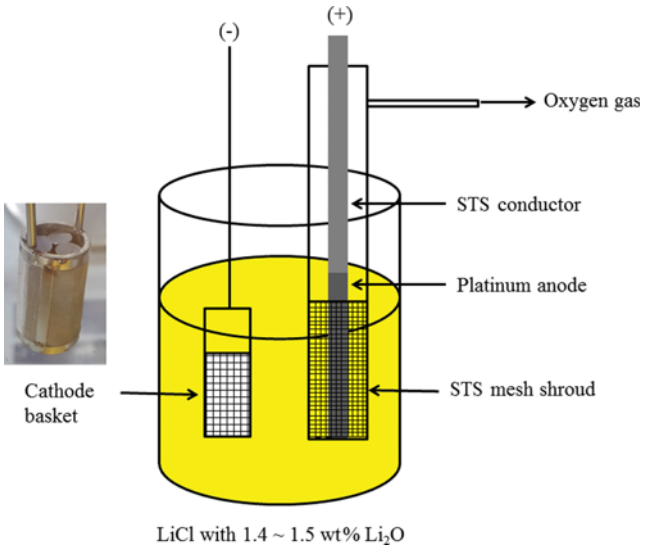

Fig. 1. Schematic diagram of the electrochemical cell employed for the electrolytic reduction reaction of porous UO_2 pellets. A picture of the cathode basket holding nine pellets is also shown.

tion of the input material for the subsequent cathode processing and electro-refining process.

EXPERIMENTAL

A schematic diagram of the electrochemical cell employed for the experiments is shown in Fig. 1. A stainless steel meshed basket was employed as the cathode where nine porous UO_2 pellets (avg. 15.7 g) were loaded as a reactant (Fig. 1). A platinum plate was employed as the anode electrode, which was covered by a stainless steel meshed shroud to collect oxygen gas. The STS shroud has a port connected to a vacuum pump so that the oxygen gas can be removed from the system as soon as possible. LiCl was employed as a salt with a Li_2O concentration of 1.4-1.5 wt%. A PC-controlled power supply (Agilent E3633A) was employed to apply electric charges into the cell. The amount of applied charges was controlled by varying the number of cycles, where one cycle consists of 30 minutes of 3.2 V cell potential and 10 minutes of power-off. The experiments were conducted for various applied charges of up to 45,000 C, and the UO_2 pellets were recovered after each experiment. The UO_2 pellets were cut into half and polished to determine the degree of reduction by measuring the radius of the inner oxide part. As the radius of remaining oxide part is dependent on the cutting position, the middle point of each pellet was cut for consistent evaluation.

The preparation method for porous UO_2 pellets was previously introduced [13,14]. Briefly, U_3O_8 powder was mixed with 0.2 wt% of acrowax lubricant (ethylene bis-stearamide, $C_{38}H_{76}O_2N_2$) and then pelletized into a cylindrical shape (6 mm diameter and 8 mm height). The pellets were heat treated at 700 °C under vacuum and maintained at this temperature for 1 h to remove the lubricant. The pellets were further heated to 1,350 °C and maintained for 12 h under a reducing atmosphere (4% H_2-Ar) to liberate oxygen atoms from U_3O_8 to produce UO_2. The resulting porous UO_2 pellets exhibited 7.65 mm in height, 5.74 mm in diameter, and 8.79 g/cm^3 in density (80.2% of theoretical density).

The concentration of Li-Li_2O around the pellets was measured by immersing the pellets in de-ionized water to dissolve LiCl salt, Li, and Li_2O. After being immersed for two days, the pellets were removed from the water and dried under a vacuum. The amount of LiCl including Li and Li_2O was determined by measuring the weight change before and after the immersion (and drying). The concentration of Li-Li_2O was analyzed by HCl titration technique using an auto-titrator (G20, Mettler Toledo). Note that the HCl titration technique cannot distinguish Li and Li_2O because both of them are reactive with water to produce LiOH. The LiOH in the salt-water solution reacts with HCl to produce LiCl and H_2O, leading to a decrease of pH. Therefore, the amount of HCl consumed to neutralize the salt solution reveals the amount of LiOH. In this study, the concentration of Li-Li_2O implies the concentration of Li in both forms of Li and Li_2O.

RESULTS AND DISCUSSION

Fig. 2 shows the cross-sectional views of the UO_2 pellets reduced by various applied charges (Q), which was controlled by the number of cycles as noted above. It is clearly seen in the figure that the radius of UO_2 shrinks with increasing Q. The term 'degree of reduc-

Q	9,640	16,400	23,000	28,800	32,200
No. cycles	2	4	7	8	10
	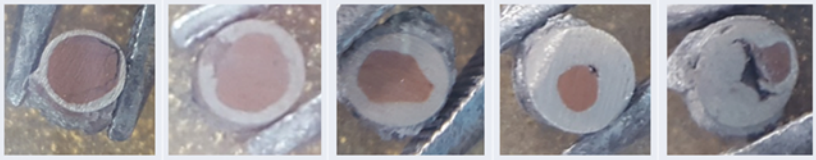				
α	0.313	0.437	0.555	0.835	0.873

Fig. 2. The pictures of cross-sections of UO_2 pellets reduced with various applied charges (controlled by number of cycles) and α values evaluated from the cross-sectional views.

tion' was defined as follows to quantify the ratio between reduced and oxide parts:

$$\alpha = 1 - \left(\frac{r}{r_0}\right)^2 \quad (1)$$

where r_0 is the radius of a whole pellet and r is the radius of remaining oxide part. As shown, the oxide part is not perfectly circular, so an average value was employed for the calculation. Interestingly, in Fig. 2 the remaining oxides are positioned off-centered especially for higher applied charges. One reason to account for this behavior is an asymmetric concentration distribution of Li metal around the pellets. In the beginning of the reduction reaction, an electrical current is applied to a metal basket surrounding the pellets. In other words, metallic lithium will be generated along the basket surface and the center of the basket will have a relatively low Li concentration compared to the surface of the basket. The Li concentration gradient inside the basket might not occur if Li generated on the basket surface is well dispersed or dissolved in the LiCl salt. The asymmetric concentration distribution of Li metal also can come from the distance between the pellets and the platinum anode electrode. As the cathode basket has cylindrical shape and platinum is located apart, the pellets positioned close to the platinum anode might have more chances to be reduced than the pellets on the opposite side. In both cases, the experimental results suggest that the diffusion or dispersion of Li is slow, resulting in a concentration gradient within the cathode basket. There is one more thing to be discussed here. As UO_2 is converted into metallic U, the metallic part of the pellets might have low electrical resistance and work as a conductor to produce Li metal on its surface. This behavior will contribute to diminishing the Li concentration gradient inside the basket, but the asymmetric shape of the remaining UO_2 at large applied charges suggests that Li metal generation is dominant at the basket surface.

The Q-α graph is shown in Fig. 3(a). In a solid-state reaction system without an identified reaction model, the Sharp-Hancock plot is a reasonable approach to verify a suitable geometry function [15]. In a Sharp-Hancock plot, a region with a linear fitting means the region shares an identical reaction mechanism, and the slope of the linear line is an indicator of the reaction model. The Sharp-Hancock plot of Fig. 3(a) is shown in Fig. 3(b) with linear fitting results. The linear fitting was valid within the range of $0 \le \alpha \le 0.56$, suggesting that they exhibit an identical reaction mechanism. At a higher α region, a linear fitting was not applicable, suggesting a change of reaction mechanism. As it is normally accepted that the Sharp-Hancock plot is available at up to 0.5-0.6 of α, the fitting results look reasonable. The fitting results of Fig. 3(b) show that the linear line exhibits a slope of 0.88, and the most appropriate reaction models were selected as the first-order (F1, slope=1.00), contracting area (R2, slope=1.07), and 1-D diffusion (D1, slope= 0.62) models [16,17]. Here, the F1 model describes a reaction that is proportional to a fraction of remaining reactant (fraction of UO_2= $1-\alpha$) with a particular power (reaction order). The R2 model represents shrinkage of cylindrically shaped reactant (UO_2 pellet in the present work) as the reduction reaction proceeds. The 1-D diffusion model assumes that the reaction is solid-state diffusion controlled and the reaction rate decreases with increasing thickness of the product barrier. In other words, the distance that metallic Li and its reaction product (Li_2O) should diffuse along the U metal layer increases with increasing α, and the diffusion rate is the rate-determining step in the D1 model. The fitting results for each

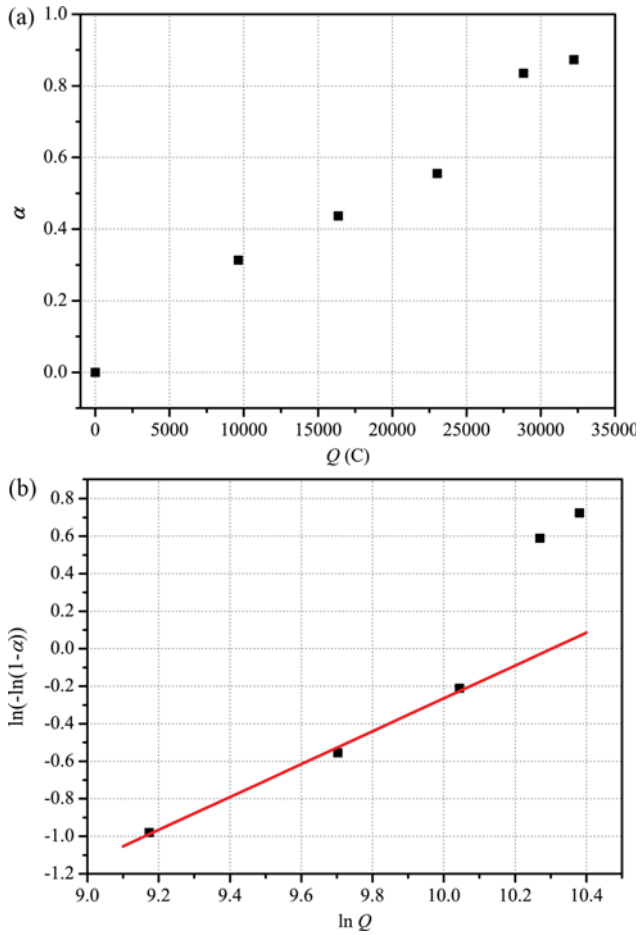

Fig. 3. (a) The Q-α graph. (b) The Sharp-Hancock plot of (a) (dots), and linear fitting results for the first three cases (red line).

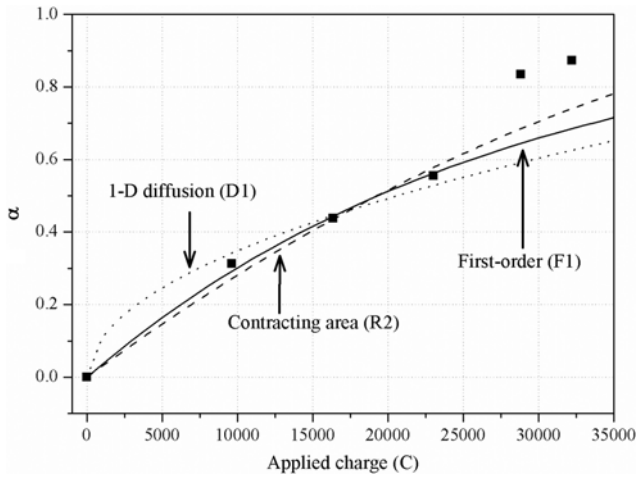

Fig. 4. The fitting results conducted using the first-order (F1), contracting area (R2), and 1-D diffusion (D1) models.

reaction model are shown in Fig. 4, and the best fitting result was achieved with the F1 model within the range of $0 \le \alpha \le 0.56$. The reduction rate of porous UO_2 pellets can be expressed as follows:

$$\alpha = 1 - EXP[-(3.59 \times 10^{-5} \times Q)] \quad (0 \le \alpha \le 0.56) \tag{2}$$

where Q represents the amount of applied charge in the unit of C. However, the F1 model is only available within the range of $0 \le \alpha \le 0.56$, and a significant mismatch at a higher α region is also shown in Fig. 4. It is meaningful that the F1 model was identified as the most suitable model for the reduction reaction of porous UO_2 pellets because the cross-sectional views (Fig. 2) were supportive of (solid-state) diffusion models. In the diffusion model, the diffusion rate of metallic lithium from the surface of the pellet into the surface of unreacted UO_2 part is the rate-determining step. However, the results of this work suggest that the porosity of the UO_2 pellets can eliminate the effect of solid-state diffusion leading to the F1 model as the most suitable one.

As mentioned in the Introduction, KAERI is greatly interested in a scale-up of the ER system. However, the reduction rate equation of Eq. (2) cannot inform us how long it will take to complete the reduction reaction when we have partially reduced products in a large system. A power law equation was used to fit the experimental results in a full range of α. A power law equation is expressed as

$$\alpha = A \times Q^n \tag{3}$$

where A is a constant and n represents the reaction order. Eq. (3) can be rewritten as

$$\ln(\alpha) = \ln(A) + n \cdot \ln(Q) \tag{4}$$

Fig. 5(a) shows the fitting results of Eq. (4), resulting in A and n values of 9.944×10^{-5} and 0.871, respectively. The fitting results were applied for the Q-α graph of Fig. 2, and it was revealed that an applied charge of 39,300 C is required for a complete reduction. In a following experiment, porous UO_2 pellets were reduced for an applied charge of 38,800 C and complete reduction was confirmed, as shown in Fig. 5(b). Thus, the following Eq. (5) might be helpful in estimating the complete reduction time in scaled-up systems.

$$\alpha = 9.944 \times 10^{-5} \times Q^{0.871} \quad (0 \le \alpha \le 1.0) \tag{5}$$

Note that the charge of 38,800 C is equal to 173% of theoretical charges for the complete reduction of UO_2 pellets (avg. 15.7 g) employed in this work. The over-charge of 73% can be rationalized by the amount of metallic Li that did not participate in the chemical reaction, including Li metal generated on the outer surface of cathode baskets. It is expected that the Li metal on the outer surface will diffuse into bulk salt because the concentration of Li metal might be higher inside the basket than in the bulk salt.

The results of the Li-Li_2O concentration, meaning Li concentration in both forms of Li and Li_2O, are shown in Fig. 6 for various amounts of applied charges. Overall, the concentration of Li-Li_2O increased with increasing Q, although the values were relatively low for the cases of 23,000 and 32,300 C, which were conducted with 600 g of LiCl salt, while the other experiments were conducted with 450 g of salt. In other words, when the concentration of 4.3 wt% at an applied charge of 23,000 C is simply modified by (600 g/450 g), the concentration is changed to 5.7 wt%. This value is still signifi-

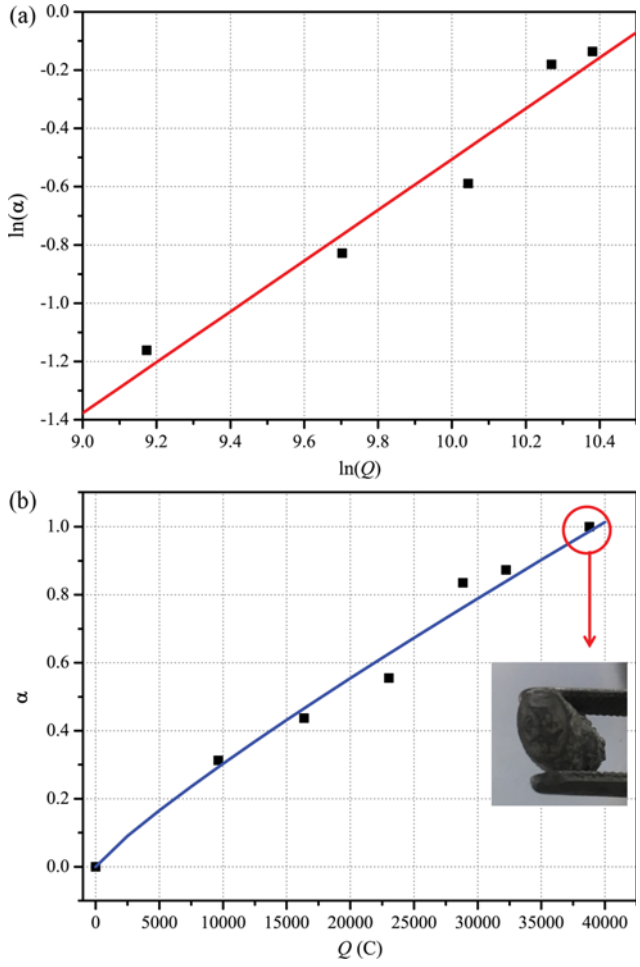

Fig. 5. (a) The ln(Q)-ln(α) graph (dots) and the linear fitting result (red line). (b) The final fitting results conducted using Eq. (5) and the cross-sectional picture of a porous UO_2 pellet reduced by an applied charge of 38,800 C.

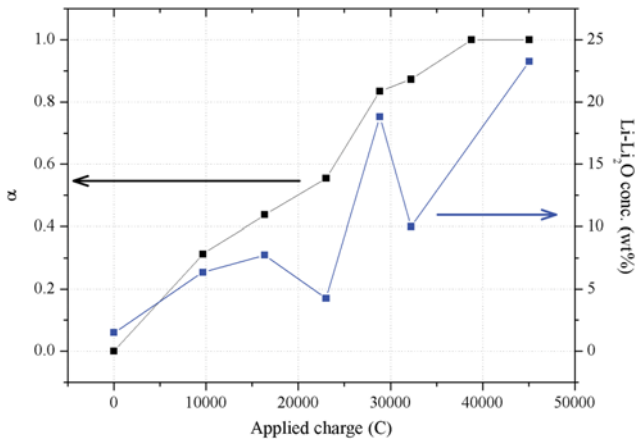

Fig. 6. Changes of α and Li-Li_2O concentration for increasing Q values. The experiments at 23,000 and 32,300 C were conducted with 600 g of LiCl salt while the others were done with 450 g of LiCl.

cantly lower than 7.7 wt% at 16,000 C and 18.8 wt% at 28,800 C, which means that an increase in the amount of salt will lead to a decrease in the concentration of Li-Li_2O near the cathode electrode. Thus, the amount of salt should be optimized to minimize the diffusion of metallic Li into bulk salt while keeping the high diffusion rate of oxygen ions. Recall that, according to the diffusion rate equations, an increasing concentration of Li-Li_2O will accelerate their diffusion into bulk salt. However, the Li-Li_2O concentration increased without a sign of deceleration, which means that the diffusion of Li-Li_2O into bulk salt is much slower than the generation rate of Li-Li_2O. Presumably, the low solubility of metallic Li (1.8 at%=0.29 wt%) and Li_2O (~8.5 wt%) in LiCl have contributed to the slow diffusion [18]. This result suggests that a cathode basket should be designed to minimize the distance between UO_2 pellets and electrical conductors for the efficient use of metallic Li. Interestingly, the observed Li-Li_2O concentration values up to 23 wt% are much higher than the solubility values of Li and Li_2O. It is suspected that the excess amount of Li-Li_2O originated from precipitates of Li_2O and/or Li. In addition, we must emphasize that uranium pellets of high Li-Li_2O concentration of up to 23 wt% will be transferred to the subsequent cathode processing and electro-refining process.

CONCLUSIONS

The electrolytic reduction reaction rate of porous UO_2 pellets was investigated for various applied charges, and the first-order reaction model was identified as the best geometry function that describes the reaction system. As the first-order reaction model shown below was available in a limited region of α,

$$\alpha = 1 - \mathrm{EXP}[-(3.59\times10^{-5}\times Q)] \quad (0 \le \alpha \le 0.56)$$

a power law type equation was also suggested for the whole range of α as below.

$$\alpha = 9.944\times10^{-5}\times Q^{0.871} \quad (0 \le \alpha \le 1.0)$$

The experimental results of the off-centered position of remaining UO_2 parts and increasing Li-Li_2O concentration with increasing applied charge suggest that the diffusion of Li into bulk LiCl salt is much slower than the generation rate, and the distance between UO_2 pellets and electrical conductors should be minimized to achieve high efficiency in a scaled-up ER system.

ACKNOWLEDGEMENT

This research was sponsored by the Nuclear R&D program of the Korean Ministry of Science, ICT & Future Planning (No. 2012M2A8A5025697).

REFERENCES

1. C. E. Stevenson, *The EBR-II fuel cycle story*, American Nuclear Society, Inc., Illinois (1987).
2. K. McMahon, P. Swift, M. Nutt, J. Birkholzer, W. Boyle, T. Gunter, N. Larson, R. MacKinnon and K. Sorenson, *J. Nucl. Fuel Cycle Waste Technol.*, **1**, 29 (2013).
3. M. J. Song, *J. Nucl. Fuel Cycle Waste Technol.*, **1**, 1 (2013).
4. K.-C. Song, H. Lee, J.-M. Hur, J.-G. Kim, D.-H. Ahn and Y.-Z. Cho, *Nucl. Eng. Technol.*, **42**, 131 (2010).
5. H. Lee, G.-I. Park, K.-H. Kang, J.-M. Hur, J.-G. Kim, D.-H. Ahn, Y.-Z. Cho and E. H. Kim, *Nucl. Eng. Technol.*, **43**, 317 (2011).
6. G. Z. Chen, D. J. Fray and T. W. Farthing, *Nature*, **407**, 361 (2000).
7. J.-M. Hur, S. M. Jeong and H. Lee, *Electrochem. Commun.*, **12**, 706 (2010).
8. S. M. Jeong, H.-S. Shin, S.-S. Hong, J.-M. Hur, J. B. Do and H. S. Lee, *Electrochim. Acta*, **55**, 1749 (2010).
9. E.-Y. Choi, J.-K. Kim, H.-S. Im, I.-K. Choi, S.-H. Na, J. W. Lee, S. M. Jeong and J.-M. Hur, *J. Nucl. Mater.*, **437**, 178 (2013).
10. W. Park, J.-M. Hur, S.-S. Hong, E.-Y. Choi, H. S. Im, S.-C. Oh and J.-W. Lee, *J. Nucl. Mater.*, **441**, 232 (2013).
11. E.-Y. Choi and S. M. Jeong, *Prog. Nat. Sci. Mater. Int.*, **25**, 572 (2015).
12. L. N. Squires and P. Lessing, *J. Nucl. Mater.*, **471**, 65 (2016).
13. E.-Y. Choi, J.-M. Hur, I.-K. Choi, S. G. Kwon, D.-S. Kang, S. S. Hong, H.-S. Shin, M. A. Yoo and S. M. Jeong, *J. Nucl. Mater.*, **418**, 87 (2011).
14. S.-C. Jeon, J.-W. Lee, J.-H. Lee, S.-J. Kang, K.-Y. Lee, Y.-Z. Cho, D.-H. Ahn and K.-C. Song, *Adv. Mater. Sci. Eng.*, **2015**, 376173 (2015).
15. J. D. Hancock and J. H. Sharp, *J. Am. Ceram. Soc.*, **55**, 74 (1972).
16. J. Szekely, J. W. Evans and H. Y. Sohn, *Gas-solid reactions*, Academic Press, New York, USA (1976).
17. A. Khawam and D. R. Flanagan, *J. Phys. Chem. B*, **110**, 17315 (2006).
18. J. Liu and J.-C. Poignet, *J. Appl. Electrochem.*, **20**, 864 (1990).